

The O₂-scavenging Flavodiiron Protein in the Human Parasite *Giardia intestinalis**[§]

Received for publication, July 9, 2007, and in revised form, October 9, 2007. Published, JBC Papers in Press, December 12, 2007, DOI 10.1074/jbc.M705605200

Adele Di Matteo, Francesca Maria Scandurra, Fabrizio Testa, Elena Forte, Paolo Sarti, Maurizio Brunori, and Alessandro Giuffrè¹

From the Department of Biochemical Sciences, CNR Institute of Molecular Biology and Pathology and Istituto Pasteur-Fondazione Cenci Bolognetti, Sapienza, University of Rome, Rome I-00185, Italy

The flavodiiron proteins (FDP) are widespread among strict or facultative anaerobic prokaryotes, where they are involved in the response to nitrosative and/or oxidative stress. Unexpectedly, FDPs were fairly recently identified in a restricted group of microaerobic protozoa, including *Giardia intestinalis*, the causative agent of the human infectious disease giardiasis. The FDP from *Giardia* was expressed, purified, and extensively characterized by x-ray crystallography, stopped-flow spectroscopy, respirometry, and NO amperometry. Contrary to flavorubredoxin, the FDP from *Escherichia coli*, the enzyme from *Giardia* has high O₂-reductase activity (>40 s⁻¹), but very low NO-reductase activity (~0.2 s⁻¹); O₂ reacts with the reduced protein quite rapidly (milliseconds) and with high affinity (K_m ≤ 2 μM), producing H₂O. The three-dimensional structure of the oxidized protein determined at 1.9 Å resolution shows remarkable similarities with prokaryotic FDPs. Consistent with HPLC analysis, the enzyme is a dimer of dimers with FMN and the non-heme di-iron site topologically close at the monomer-monomer interface. Unlike the FDP from *Desulfovibrio gigas*, the residue His-90 is a ligand of the di-iron site, in contrast with the proposal that ligation of this histidine is crucial for a preferential specificity for NO. We propose that in *G. intestinalis* the primary function of FDP is to efficiently scavenge O₂, allowing this microaerobic parasite to survive in the human small intestine, thus promoting its pathogenicity.

The flavodiiron proteins (FDP,² originally named A-type flavoproteins (1)) are widespread among Bacteria and Archaea,

either strict or facultative anaerobes, where they have been proposed to play a role in the response to nitrosative and/or oxidative stress (2, 3). A few prokaryotic FDPs have been characterized to date, namely those from the bacteria *Desulfovibrio gigas* (originally named rubredoxin:oxygen oxidoreductase, ROO (4–7), and hereafter denoted FDP_{Dg}), *Escherichia coli* (named flavorubredoxin, FIRd,³ Refs. 2, 8–11), *Desulfovibrio vulgaris* (12), *Moorella thermoacetica* (FDP_{Mt} (13, 14)), and the homologous enzyme from the methanogenic archaeon *Methanothermobacter marburgensis* (FDP_{Mm}, Refs. 15, 16). The FDPs contain two redox centers: a FMN, the electron entry site into the enzyme, and a non-heme Fe-Fe center, the active site (13). They are cyanide-insensitive enzymes able to catalyze the reduction of O₂ (to H₂O) and/or NO (to N₂O). Some of these enzymes are almost exclusively reactive toward NO (such as *E. coli* FIRd, Refs. 2, 9),⁴ others toward O₂ (such as the *M. marburgensis* enzyme, (15)), whereas some FDPs catalyze the reduction of both gases, though with different efficiency (7, 12, 13). These enzymes are expected to play a protective role in anaerobic or microaerobic microorganisms that need to survive under O₂ and cope with NO produced by the host defense system to counteract infection (17, 18).

Surprisingly, a few years ago, genes coding for FDPs were identified also in the genome of a few eukaryotes, namely some amitochondriate microaerobic protozoan parasites including *Giardia intestinalis*, *Trichomonas vaginalis*, *Spironucleus barkhanus*, *Mastigamoeba balamuthi*, and several *Entamoeba* strains (19–22). Despite their potential pathophysiological relevance, structural and functional information on eukaryotic FDPs is still marginal.

G. intestinalis is the causative agent of giardiasis, a widespread intestinal infectious disease in humans (23). Very recently, its genome has been completely sequenced (24), lead-

* This work was supported in part by Ministero dell'Università e della Ricerca of Italy (PRIN Meccanismi molecolari e aspetti fisiopatologici dei sistemi bioenergetici di membrana (to P. S.) and FIRB RBLA03B3KC_004 (to M. B.)) and by Consiglio Nazionale delle Ricerche of Italy (CNR-GRICES joint project (to A. G.)). The costs of publication of this article were defrayed in part by the payment of page charges. This article must therefore be hereby marked "advertisement" in accordance with 18 U.S.C. Section 1734 solely to indicate this fact.

The atomic coordinates and structure factors (code 2Q9U) have been deposited in the Protein Data Bank, Research Collaboratory for Structural Bioinformatics, Rutgers University, New Brunswick, NJ (<http://www.rcsb.org/>).

[§] The on-line version of this article (available at <http://www.jbc.org/>) contains supplemental Figs. S1 and S2 and Table S1.

¹ To whom correspondence should be addressed: Istituto di Biologia e Patologia Molecolare, Consiglio Nazionale delle Ricerche c/o Dipartimento di Scienze Biochimiche, Sapienza Università di Roma, Piazzale Aldo Moro 5, I-00185, Rome, Italy. Fax: 39-06-4440062; E-mail: alessandro.giuffre@uniroma1.it.

² The abbreviations used are: FDP, flavodiiron protein; FDP_{Gt}, FDP from *G. intestinalis*; FDP_{Dg}, FDP from *D. gigas*; FDP_{Mt}, FDP from *M. thermoacetica*;

FDP_{Mm}, FDP from *M. marburgensis*; FIRd, *E. coli* flavorubredoxin; FIRd-red, NADH:flavorubredoxin oxidoreductase; Rd, genetically truncated rubredoxin domain of *E. coli* flavorubredoxin; ROS, reactive oxygen species; NO, nitric oxide; PFOR, pyruvate:ferredoxin oxidoreductase; r.m.s.d., root mean square deviation.

³ In the majority of (but not all) FDPs, the reducing substrate is rubredoxin, a small iron-sulfur protein that in turn is re-reduced by NAD(P)H via a specific FAD-containing oxidoreductase (see Ref. 3 for a review). The FDP from *E. coli* is fused to rubredoxin (hence the name flavorubredoxin, FIRd) and it is thus reduced directly by the specific reductase, the NADH:flavorubredoxin (FIRd-red, Refs. 8 and 11) oxidoreductase.

⁴ *E. coli* FIRd displays a very low O₂-reductase activity (<1 s⁻¹, J. B. Vicente, F. M. Scandurra, M. Brunori, P. Sarti, M. Teixeira, A. Giuffrè, unpublished results), largely overestimated in Ref. 9 because of the direct reaction of O₂ with the reducing substrate, NADH:flavorubredoxin oxidoreductase.

The Flavodiiron Protein from *Giardia*

ing to conclude that *Giardia* is an early diverging protozoan with very simplified metabolic pathways. Although *Giardia* has a relatively poor tolerance to O₂, it preferentially colonizes the fairly aerobic upper part of the small intestine (duodenum and jejunum). The parasite has an essentially fermentative energy metabolism (25). It lacks the conventional respiratory oxidases as well as the systems (catalase, superoxide dismutase, glutathione reductase) responsible for the scavenging of radical oxygen species (ROS) (26).

Here we present the three-dimensional structure of the FDP from *Giardia* solved by x-ray crystallography, and provide evidence that in addition to the H₂O-producing NADH-oxidase previously characterized (27), *Giardia* employs the FDP system to efficiently cope with O₂. To the best of our knowledge this is the first eukaryotic FDP characterized, to date.

EXPERIMENTAL PROCEDURES

Materials—Stock solutions of ~2 mM NO (Air Liquide, France) were prepared by equilibrating degassed water with the pure gas at 1 atm and room temperature. The concentration of *E. coli* FIRD-red and of the genetically truncated rubredoxin domain of *E. coli* flavorubredoxin (Rd) in the oxidized state was determined using $\epsilon_{455\text{ nm}} = 12\text{ mM}^{-1}\text{ cm}^{-1}$ and $\epsilon_{484\text{ nm}} = 7\text{ mM}^{-1}\text{ cm}^{-1}$, respectively.

Cloning, Expression, and Purification—The gene coding for the *G. intestinalis* FDP (FDP_{Gi})⁵, synthesized by GENEART GmbH (Regensburg, Germany), was cloned in pET28b(+) vector (Novagene). Expression of the His-tagged protein in *E. coli* BL21-Gold (DE3) cells was induced with 0.1 mM isopropyl α -D-thiogalactoside after supplementing the medium with 100 μ M ferrous ammonium sulfate (NH₄Fe(SO₄)₂·6H₂O); cells were grown at 25 °C in M9 medium. The recombinant protein was purified by Nickel affinity chromatography, followed by gel filtration chromatography to remove excess imidazole. After His tag cleavage with thrombin, the protein was subjected to a second step of nickel affinity and gel filtration chromatography.

Protein Characterization—The protein concentration was determined by the Bicinchoninic Acid Assay (BCA) (28). The FMN was quantitated according to Ref. 29 and iron using the ferrozine assay (30) (see supplemental materials for details). The quaternary structure of FDP_{Gi} in solution was determined using a TricornTM Superdex 200–10/300 HPLC column (Amersham Biosciences GE Healthcare). Stopped-flow experiments were carried out with a thermostated instrument (DX.17MV, Applied Photophysics, Leatherhead, UK) equipped with a diode-array (light path, 1 cm). Time-resolved absorption spectra were recorded with an acquisition time of 2.5 ms per spectrum. Kinetic data were analyzed by nonlinear least-squares regression analysis using the software MATLAB (MathWorks, South Natick, NA). Nitric oxide (NO) and oxygen consumption measurements were carried out using Clark-type selective electrodes (Apollo 4000 from World Precision Instruments or Oxygraph-2k from Oroboros Instruments). In these measurements, turnover numbers were estimated based on the amount of the enzyme incorporating FMN.

TABLE 1
Data collection and refinement statistics

Data collection	
Space group	P2 ₁ 2 ₁ 2
Unit cell dimensions (Å)	a = 111.97; b = 115.06; c = 67.73
Wavelength (Å)	1.0
Resolution range (Å)	80–1.9 (1.97–1.9)
Total reflections	507,268
Unique reflections	69,660
Completeness (%) ^a	98.3 (92.3)
Redundancy	7.3 (6.4)
Average I/ σ ^a	21.7 (3.7)
R _{merge} % ^a	8.7 (43.0)
Wilson B value (Å ²)	17.7
Refinement	
Resolution range (Å)	50.0–1.9
R _{cryst} %	16.6
R _{free} % ^b	20.4
Number of atoms	
Protein	6430
Waters	776
FMN, Fe, MUO, nitrate	62, 4, 2, 20
Mean B factors (Å ²)	
Protein	15.8
Waters	20.3
FMN, Fe, MUO, Nitrate	20.3, 13.2, 11.4, 27.5
R.m.s.d. bonds (Å)	0.014
R.m.s.d. angle (°)	1.393

^a Number in parentheses is for the last shell.

^b R_{free} was calculated on 5% of data excluded before refinement.

Protein Crystallization—Best crystals of FDP_{Gi} were obtained by hanging drop vapor diffusion method using the following reservoir solution: 0.1 M sodium acetate pH 4.6, 14–16% PEG 3350, and 0.2 M potassium nitrate. Drops were prepared by mixing 1.0 μ l of reservoir solution and 1.0 μ l of protein (12 mg/ml) and allowed to equilibrate against 0.5 ml of the reservoir. Crystals were cryoprotected in 0.1 M sodium acetate pH 4.6, 20% PEG 3350, 0.4 M potassium nitrate and 20% PEG 200. Diffraction data were collected at 100 K at the ID29 beamline of the ESRF Synchrotron (Grenoble, France). Data were indexed and integrated with DENZO and SCALEPACK, respectively (31). The best quality crystal diffracted up to 1.9 Å resolution (Table 1). Two molecules were found in the asymmetric unit corresponding to a solvent content of 45.4% and a V_M coefficient of 2.3.

Crystal Structure Determination and Refinement—The crystal structure of FDP_{Gi} was determined by Molecular Replacement with MOLREP (32) using the structure of the FDP from *M. thermoacetica* (PDB code 1YCF, Ref. 14) as template. A rigid body refinement with REFMAC5 (33), followed by ARP/wARP (procedure: improvement of maps by atom update and refinement), was then applied to improve the quality of the initial map. The model was built with COOT (34), iteratively refined using REFMAC5 (33), visually inspected, and manually rebuilt. Solvent molecules were added into the F_O-F_C density map. The iron atoms, the oxo (hydroxo or aquo) bridges and the nitrate ions were introduced only in the late stages of the refinement to prevent model bias. The final model was refined to R_{factor} and R_{free} equal to 16.6 and 20.4%, respectively, at 1.9-Å resolution (Table 1).

The FDP_{Gi} crystal structure consists of a total of 814 residues (residues 4–412 for monomer A and residues 6–412 for monomer B), two FMN, four Fe atoms, two oxo (hydroxo or aquo) bridges, five nitrate ions, and a total of 781 water molecules in the asymmetric unit. Residues 4, 124, 376, 387, 408, 412 of monomer A and residues 124, 216, 376, and 412 for monomer B

⁵ GenBankTM accession code 27981644.

were fitted as alanine because of the lack of density for the side chain. The refined model was checked for geometrical quality by using PROCHECK (35). Ramachandran statistics show that 99.5% of the residues lie in allowed regions, while four residues (Asp-55 and Phe-382 in both monomers) lie in disallowed regions. Asp-55 is in the proximity of the Fe-Fe center, while Phe-382 contacts FMN. The residues topologically corresponding to Asp-55 and Phe-382 lie in disallowed regions of the Ramachandran plot also in FDP_{Mt} and in generously allowed regions in FDP_{Mm}. Structural superposition was performed using SSM Superposition as implemented in COOT (36). Analysis of ligand-protein contacts was performed with SPACE (37). Figures were generated using PyMol (DeLano, W.L. The PyMOL Molecular Graphics System (2002) DeLano Scientific, San Carlos, CA). The accessible surface area was calculated with AREA-MOL (38).

The atomic coordinates have been deposited in the Protein Data Bank (www.pdb.org; PDB ID code 2Q9U).

RESULTS

General Properties of the Purified Protein

The recombinant FDP from *Giardia* (FDP_{Gi}) was purified to homogeneity with a typical yield of ~3 mg of protein *per* gram of *E. coli* cells. SDS-PAGE shows that the protein is a single polypeptide with molecular mass ~45 kDa, consistent with the value of 46,904 Da calculated from the amino acid sequence. HPLC analysis (not shown) indicates that in solution the protein is a tetramer with an apparent molecular mass of 169 ± 17 kDa. As purified, each monomer of FDP_{Gi} contains ~1.5 Fe and ~0.5 FMN (see supplemental materials), instead of 2 Fe and 1 FMN, which implies partial loss of the cofactors during purification or incomplete incorporation during expression. The oxidized protein displays a UV/visible absorption spectrum dominated by the flavin cofactor, with bands at 358 and 461 nm. In the presence of NADH, only upon addition of catalytic concentrations of the *E. coli* proteins FIRd-red and Rd, FDP_{Gi} is reduced and absorption in the visible region almost completely bleached (see *dashed spectra* in Fig. 1).

The Function

Kinetics of Oxidation by O₂ and NO—The reactivity of reduced FDP_{Gi} with O₂ and NO was tested at 20 °C by stopped-flow absorption spectroscopy. As shown in Fig. 1 (*top panel*) the reduced protein is very rapidly oxidized even by a 2-fold excess of O₂, suggestive of a high affinity; ~80% of the protein is oxidized with a *t*_{1/2} ~3 ms, the remainder being oxidized on a much longer time scale (a few seconds). As the stopped-flow instrument collects spectra every 2.5 ms, the fast oxidation of the large majority of the protein is at the limits of the time resolution of the technique, proceeding at an estimated second order rate constant *k* > 10⁷ M⁻¹ s⁻¹. The protein is instead oxidized by H₂O₂ much more slowly (*k* = 1.7 s⁻¹ at [H₂O₂] = 60 μM, not shown), ruling out a peroxidatic activity for FDP_{Gi}.

Compared with O₂, the protein is much less reactive toward NO, being oxidized only within seconds even at very high NO concentrations. For instance, at [NO] = 650 μM, the oxidation of FDP_{Gi} followed under strictly anaerobic conditions, proceeds at *k* = 2.7 s⁻¹ (Fig. 1, *bottom panel*), the reaction being

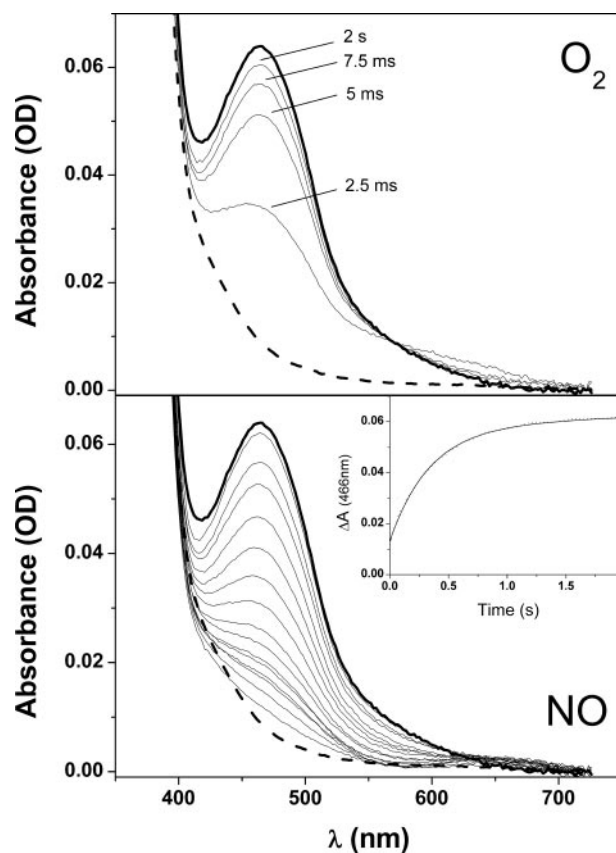


FIGURE 1. Kinetics of the reaction of FDP_{Gi} with O₂ or NO. FDP_{Gi} was pre-reduced by incubation with an excess of NADH and small amounts of FIRd-red and Rd, and mixed in the stopped-flow apparatus with O₂ (*top*) or NO (*bottom*). Concentrations after mixing: [FDP_{Gi}] = 6.7 μM; [NADH] = 150 μM; [FIRd-red] = 100 nM; [Rd] = 250 nM; [O₂] = 14 μM (*top*) or [NO] = 650 μM (*bottom*). Buffer: 50 mM Tris, 18% glycerol, pH 7.5. *T* = 20 °C. Bold spectra: fully reduced (*dashed*) and end-point oxidized (*solid*) species. At λ < 400 nm, absorption is dominated by NADH. *Top*, after mixing with O₂, most of the protein is oxidized within a few milliseconds. *Bottom*, as compared with O₂, the reaction with NO is much slower. Anaerobic conditions achieved by extensively degassing the buffer, prior to addition of 2 mM glucose, 17 units/ml glucose oxidase and 130 units/ml catalase. *Inset*, best fit to a single exponential (*k* = 2.7 s⁻¹) of the reaction with NO at λ = 466 nm.

even slower at lower NO concentrations. Under anaerobic conditions, low molecular weight nitrosothiols, such as nitroso-cysteine, can also oxidize FDP_{Gi}, although at very low rate (*k* = 0.1 s⁻¹ at 50 μM nitroso-cysteine, not shown).

O₂ and NO Amperometric Measurements—The ability of FDP_{Gi} to catalyze the consumption of O₂ or NO was tested by using selective electrodes. In these assays, a large excess of NADH (1 mM) was used as the primary electron donor, and the *E. coli* proteins FIRd-red and Rd were added to shuttle electrons to FDP_{Gi}. As shown in Fig. 2 (*top panel*), the protein displays a remarkable O₂-reductase activity with a turnover number linearly dependent on [Rd] (at least up to 20 μM) and equal to 37.7 ± 8.3 s⁻¹ at [Rd] = 20 μM (*inset* to Fig. 2, *top panel*); as expected, the activity vanishes upon FDP_{Gi} denaturation, as well as if the reducing substrate, Rd, is omitted (not shown). Addition of catalase has no effect on the apparent rate of O₂ consumption, pointing to H₂O (and not H₂O₂) as the reaction product: consistently, by monitoring NADH oxidation at 340 nm in control experiments, we measured a NADH/O₂ stoichiometry equal to 2 (not shown). As shown in Fig. 2 (*top panel*),

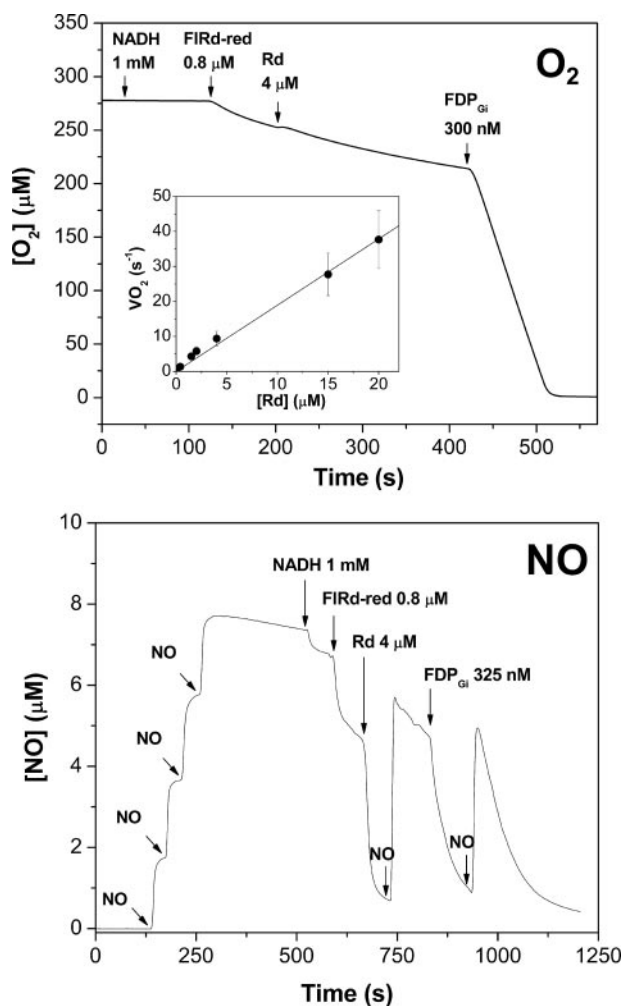


FIGURE 2. The consumption of O₂ or NO by FDP_{Gi}. Buffer: 50 mM Tris, 18% glycerol, 20 μM EDTA, pH 7.5. *T* = 20 °C. *Top*, NADH and *E. coli* FIRd-red and Rd are added in sequence to an air-equilibrated solution. Following the addition of FDP_{Gi}, O₂ is promptly consumed at ~7.8 s⁻¹. *Inset*, oxygen turnover number of FDP_{Gi} as a function of [Rd]. *Bottom*, four aliquots of NO are added in sequence to the anaerobic buffer, yielding ~8 μM NO in solution. Following the addition of NADH and *E. coli* FIRd-red and Rd, NO is totally consumed and thus re-added in solution. The subsequent addition of FDP_{Gi} causes only a modest increase in NO consumption (~0.2 s⁻¹), evident also after re-addition of NO to the solution. Anaerobic conditions achieved by adding 5 mM sodium ascorbate and 13 μg/ml ascorbic oxidase to the degassed buffer.

O₂ consumption follows zero order kinetics down to at least 10 μM O₂. Below this concentration, the time course of O₂ consumption deviates from linearity due to O₂ limitation: analysis of this non-linear part of the time course yields an apparent $K_m \leq 2 \mu\text{M}$. Contrary to other members of the FDP family (12, 13), no irreversible inactivation of the *Giardia* enzyme is observed during turnover with O₂, unless catalase is omitted in the assay; in the latter case, H₂O₂ produced by the reaction of FIRd-red with O₂ slowly, but progressively inhibits the enzyme (not shown).

Similar experiments have been carried out to test also the NO-reductase activity of FDP_{Gi} under anaerobic conditions (Fig. 2, bottom panel). In the absence of FDP_{Gi} a significantly enhanced consumption of NO is observed after addition of Rd in the presence of NADH and FIRd-red; however, if NO is re-added to the solution, following the addition of FDP_{Gi} con-

sumption of NO proceeds at a turnover rate of only ~0.2 s⁻¹. Moreover, this low rate of NO consumption was found to be essentially independent of the concentration of Rd. In conclusion, FDP_{Gi} displays high O₂-reductase activity, but very low NO-reductase activity, in agreement with the stopped-flow data described above.

The Three-dimensional Structure

The crystal structure of FDP_{Gi} was solved at 1.9-Å resolution. The asymmetric unit contains two monomers forming a non-physiological dimer that yields a tetramer by applying crystallographic symmetry. Such a tetramer consists of a dimer of dimers (Fig. 3A) and possibly represents the assembly of the protein in solution, as indicated by the HPLC data (see above). Upon formation of the physiological dimer ~10.9% of the ASA of each monomer becomes buried, whereas the ASA of each dimer decreases by ~12.9% in the tetrameric assembly. Interestingly, a similar homotetrameric arrangement has been reported for FDP_{Mm} (16), but not for the homologous enzymes from *D. gigas* (6) and *M. thermoacetica* (14), whose structures were also solved; the latter two proteins were indeed reported to be dimers.

The two monomers in the asymmetric unit are completely superimposable (with a r.m.s.d. value calculated on the equivalent Cα atoms of 0.13 Å). Each monomer is composed of two domains: a N-terminal β-lactamase-like domain containing the Fe-Fe center and a C-terminal flavodoxin-like domain containing the FMN cofactor (Fig. 3B): inspection of the Fo-Fc electron density maps reveals that the cofactor content is compatible with 0.8–1.0 FMN and 1.9–2.0 Fe per monomer. The β-lactamase-like domain (residues 4–252 for chain A and 6–252 for chain B) contains a sandwich of two β-sheets, each flanked on its outer face by three α-helices, and a two-stranded β-sheet that protrudes out from the central sandwich covering the Fe-Fe site. The flavodoxin-like domain (residues 253–412) contains five parallel β-strands, forming a central β-sheet surrounded on both sides by a total of five α-helices. Overall, the structure of FDP_{Gi} and those available for bacterial flavodiiron proteins are similar (rmsd calculated on Cα equivalent atoms of the dimers equal to 1.71, 1.7, and 1.84 Å for FDP_{Dg}, FDP_{Mp} and FDP_{Mm}, respectively).

Within each monomer the distance between the FMN and the Fe-Fe center is much too long (about 40 Å) to allow fast electron transfer between the two redox centers. In the physiological dimer, however, the monomers are in a head to tail arrangement that brings the Fe-Fe cluster of one monomer close to the FMN of the other one, thus allowing efficient electron transfer (Fig. 3A).

Three regions of the protein sequence account for most of the FMN contacts, namely the residues ²⁶⁵SMYGT²⁷⁰, ³¹⁶PTLNN³²⁰, ³⁴⁹AFGWS³⁵³, and F382. The aromatic ring of Trp-352 is co-planar with the FMN isoalloxazine ring. This residue, almost conserved in FDPs, is likely involved in shuttling electrons between rubredoxin and FMN (16), and has been proposed (3) to account for the broadness of the 450 nm absorption band observed in most of the FDPs characterized so far. Additionally, the FMN moiety is contacted by a few residues of the nearby monomer (His-31, Glu-87, His-152, Trp-153, Ile-203, Leu-206, and Phe-207). His-31 is conserved in FDP_{Mt} and

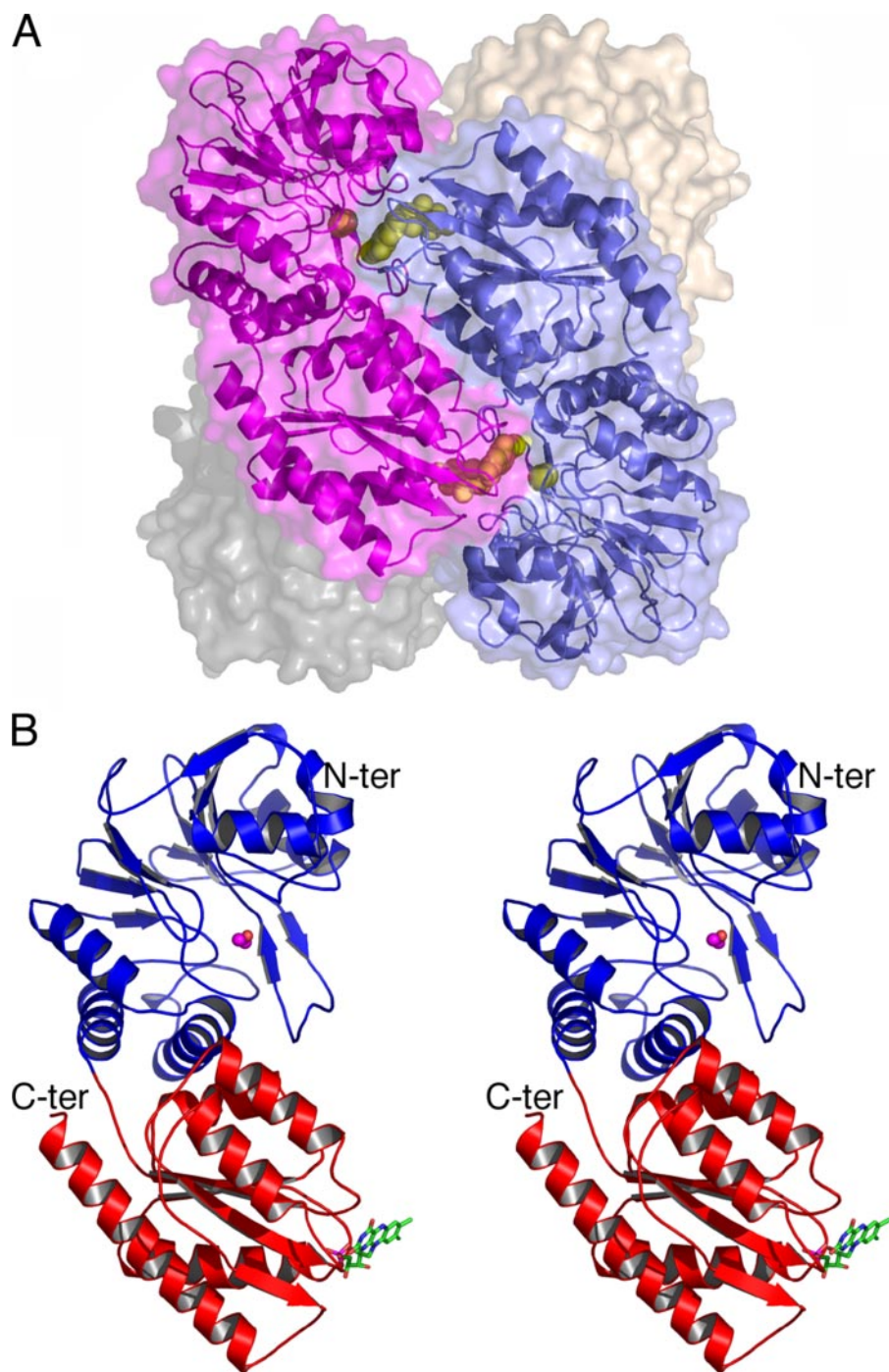


FIGURE 3. **Overall structure of FDP_{Gi}.** *A*, tetrameric protein is shown as a transparent surface, with one of the functional dimers highlighted in ribbon representation (slate and magenta colors for the two monomers). FMN and the di-iron site depicted as yellow spheres. *B*, stereo view of one FDP_{Gi} monomer in ribbon presentation with the N-terminal β -lactamase-like and the C-terminal flavodoxin-like domains colored in blue and red, respectively. FMN is represented in green sticks, the Fe atoms and the oxo (hydroxo or aquo) bridge as magenta and orange spheres, respectively.

in FDP_{Mm}, but it is replaced in its topological position by a Tyr residue in FDP_{Dg} (see below). Glu-87, His-152, and Trp-153 are conserved among all FDP structures solved to date. Notably, both Glu-87 and His-152 are involved also in iron coordination (see below). In particular the C8M of FMN is about 3.5 Å far from the OE2 atom of Glu-87.

Similarly to FDP_{Dg}, FDP_{Mt} and FDP_{Mm}, the active site of FDP_{Gi} contains two irons (Fe1 and Fe2, the nearest to FMN) at

a short distance (3.46 and 3.55 Å in each monomer) with an oxo (hydroxo or aquo) bridge, that is a common feature for di-iron proteins (39). Fe1 is ligated by the NE2 atoms of His-90 (2.14 Å) and His-230 (2.18 Å), by the OD2 atom of D89 (2.08 Å) and by the OD1 of Asp-171 (2.09 Å), the latter aspartate bridging the two iron atoms and coordinating Fe2 through the OD2 atom (2.08 Å). Fe2 is also coordinated by the NE2 of His-85 (2.29 Å), the NE2 of His-152 (2.14 Å) and the OE1 of Glu-87 (2.14 Å); the two latter residues are also involved in FMN binding. The oxo bridge is located at 1.94 and 1.97 Å from the Fe1 and Fe2, respectively. A *cis* peptide bond is present between Leu-151 and His-152, also detected in FDP_{Dg} and in the active reduced form of FDP_{Mm} (but not in FDP_{Mt}), and proposed to be necessary to project the imidazole ring of His-152 toward Fe1 (16). His-152 is located in a loop (Pro-149–Pro-154) referred to as the switch loop in FDP_{Mm}, where it undergoes a redox conformational change opening the binding site for the F₄₂₀H₂ cofactor (16).

Fig. 4A shows a superposition of the Fe-Fe site coordination sphere of FDP_{Mt}, FDP_{Dg}, and FDP_{Mm} in the active form. All ligand residues occupy similar positions with the notable exception of the residue His-84 in FDP_{Dg} (equivalent to His-90 in FDP_{Gi}). In FDP_{Dg} this residue is stabilized in a non-bonding “out conformation” by interacting with an aspartate (Asp-225 in FDP_{Dg}), that is replaced by alanine or serine in all the other FDP structures solved to date, including FDP_{Gi}; consistently, in the latter enzymes this histidine residue coordinates the Fe atom. This structural difference was originally proposed (14) to account for the different

specificity displayed by FDPs toward O₂ or NO. However, as discussed below, also based on our results, this hypothesis seems unlikely.

By inspection of the electron density map, a cloud of density is detected above the Fe-Fe center (Fig. S1 in supplemental data), compatible with an acetate or nitrate ion, both present in the crystallization medium. Such density was

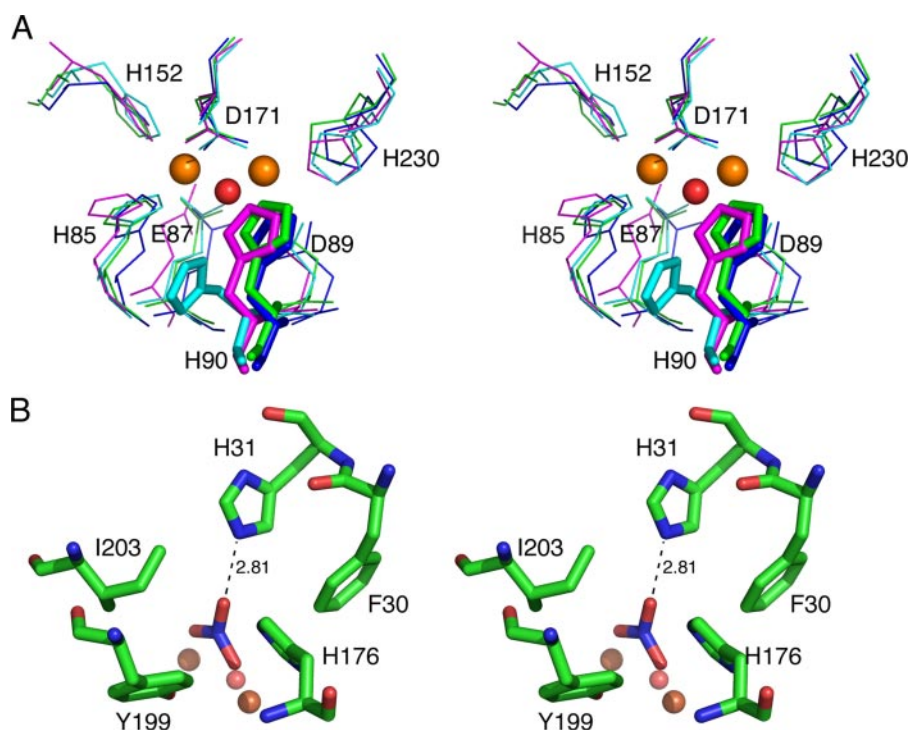


FIGURE 4. **The Fe-Fe site and the putative O₂ binding pocket.** *A*, stereo view of the Fe-Fe site coordination sphere in FDP_{Gi} (green), FDP_{Dg} (cyan), FDP_{Mt} (magenta), and FDP_{Mm} (blue), with the Fe atoms and the oxo (hydroxo or aquo) bridge depicted as orange and red spheres, respectively. Notice that His-90 (FDP_{Gi} numbering) is Fe-ligated in all FDPs except in the *D. gigas* enzyme. *B*, stereo view of the putative O₂ binding pocket of FDP_{Gi}. Residues surrounding the putative O₂ binding pocket with the nitrate represented in sticks and the H-bond with the NE2 atom of His-31 highlighted (see text).

interpreted as a nitrate since this ion can make an additional H-bond with the His-31 NE2 atom (2.81 Å). Nitrate is bonded to both Fe atoms, thus occupying their sixth coordination position (Fig. 4*B*). Nitrate is located in the putative O₂ binding pocket in similar position where an O₂ molecule was found in FDP_{Dg} and a H₂O, an O₂ or an ethylene glycol molecule were found in the three structures of FDP_{Mt}. In addition to the Fe ligating residues, the pocket is surrounded by five additional residues (Phe-30, His-31, His-176, Tyr-199, Ile-203) (Fig. 4*B*). Structural superposition of the putative O₂ binding pocket in FDPs (Fig. S2 in supplemental data) reveals that Tyr-199 is conserved and replaced by a phenylalanine only in FDP_{Mm}; Ile-203 is conserved or conservatively mutated, and His-176 is replaced in its topological position by an asparagine residue only in FDP_{Dg}. Major differences are located above the pocket in the loop containing Phe-30 and His-31, that in FDP_{Gi} is one residue shorter than in FDP_{Dg}, two residues shorter than in FDP_{Mt} and one residue longer than in FDP_{Mm}. This difference allows His-31 to occupy the same position as His-25 in FDP_{Mt} and His-26 in FDP_{Mm}, whereas the same topological position is occupied by a tyrosine (Tyr-26) in FDP_{Dg}. Interestingly, in FDP_{Mt} mutation to phenylalanine of residues His-25 and Tyr-195 (corresponding to His-31 and Tyr-199 in FDP_{Gi}, respectively) was shown to considerably lower the NO-reductase activity of this protein (14), presumably because involved in substrate binding.

DISCUSSION

G. intestinalis is an amitochondriate, microaerophilic parasite responsible for giardiasis, a common intestinal infectious disease and an important cause of morbidity in the developing countries. The disease is transmitted through fecal-oral transfer of *Giardia* cysts, that after ingestion transform into trophozoites and colonize the small intestine; this causes various grades of symptoms, including nausea, stomach cramps, diarrhea, and vomiting, up to failure-to-thrive syndrome in children (23). Nitroimidazoles derivatives, particularly metronidazole, are widely used to treat the disease, though clinical resistance to these drugs has been repeatedly observed.

Giardia is a protozoan with an essentially glycolytic fermentative energy metabolism (25), leading to production of CO₂, ethanol, alanine, and acetate. The parasite lacks the conventional respiratory enzymes, thus producing ATP by substrate level phosphorylation only (25). Relevant to this study, *Giardia*

displays a significant sensitivity to O₂ (40), that was attributed to: (i) the expression of O₂-labile key metabolic enzymes, such as pyruvate:ferredoxin oxidoreductase (PFOR, Ref. 41) and (ii) to the reactive oxygen species (ROS) produced by reaction of O₂ with NAD(P)H:menadiol oxidoreductase (DT-diaphorase) (42). O₂ sensitivity is also enhanced by the fact that *Giardia* lacks the conventional ROS scavenging systems (26). Despite its O₂ sensitivity, *in vivo* the parasite is exposed to significant levels of O₂ in the luminal portion of duodenum and jejunum, where up to 50 μM O₂ is present (43). Therefore, the occurrence of an efficient O₂ scavenging system is strictly required for survival and pathogenicity of *Giardia*.

Cells of the parasite were shown to be endowed with an O₂ consuming activity (40, 44, 45), that was attributed to a H₂O-producing FAD-containing NADH oxidase (27). This oxidase was thus proposed to be the enzyme responsible for protection of *Giardia* from O₂.

We have investigated the structural and functional properties of the FDP from *G. intestinalis* (FDP_{Gi}). This is one of the very few eukaryotic FPDs identified by genomic analyses, presumably acquired from prokaryotes by lateral gene transfer (19–22,24). Our results clearly indicate that the enzyme displays high O₂-reductase activity with formation of H₂O (>40 s⁻¹), but very low NO-reductase activity (~0.2 s⁻¹). The rate of O₂ reduction is so high that, even at the highest concentration of the reducing substrate tested ([Rd] = 20 μM), saturation is not achieved, thus preventing an estimate of V_{max}; of course, this

may be partly due to limited efficiency of the nonphysiological reducing substrate used in the assays. In turnover with O₂, FDP_{Gi} does not display the significant inactivation reported for other FPDs (12, 13), and O₂ is consumed following zero-order kinetics up to at least 10 μM O₂. Unlike NO, O₂ was found to react with the protein not only very rapidly, but also with high affinity ($K_m \leq 2 \mu\text{M}$, Figs. 1 and 2), yielding H₂O as the product.

Based on the remarkable O₂ reactivity, we propose that FDP_{Gi} plays a crucial role for *in vivo* O₂ detoxification. It remains to be established whether FDP_{Gi} and NADH-oxidase work synergistically. In this respect, it is interesting to observe that sequence analysis of *Giardia* NADH-oxidase and FDP_{Gi} suggested to us that these two proteins may belong to the same electron transport chain, accounting for O₂ detoxification.⁶

FDP_{Gi} does not seem to be involved in *Giardia* protection from nitrosative stress, as it is endowed with only very low NO-reductase activity. NO is typically produced by the host immune system as part of the response to microbial infection (17, 18). NO exerts cytostatic, but not cytotoxic effects toward *Giardia* (46), but the parasite counteracts the NO produced by nitric-oxide synthase (NOS) by actively consuming arginine (46). More recently, it has been proposed that *Giardia* infection might be cleared by the NO-induced stimulation of gastrointestinal motility (47), rather than by direct exposure of the pathogen to NO. Based on this information, it may not be surprising that FDP_{Gi} was selected to scavenge O₂ much more efficiently than NO, unlike most of the bacterial FPDs characterized to date. A similar specificity toward O₂ was indeed reported only for the homologous protein from the methanogenic archaeon *M. marburgensis* (FDP_{Mm}) (16).

In the present study, the three-dimensional structure of the FDP from *Giardia* has been determined by crystallography (resolution 1.9 Å). The FDP_{Gi} displays a tetrameric assembly consisting of a dimer of homodimers in a head-to-tail arrangement; a similar assembly was reported for the *M. marburgensis* enzyme (FDP_{Mm}) (16), where it was proposed to deal with thermoadaptation of this archaeal microorganism.

Overall, the structure of FDP_{Gi} shows remarkable similarities with those of the few other prokaryotic members of the FDP family solved to date, namely the enzymes from *D. gigas* (FDP_{Dg}) (6), *M. thermoacetica* (FDP_{Mt}) (14), and *M. marburgensis* (FDP_{Mm}) (16). A notable difference among the available structures is at the level of the residue His-90 that is a ligand of one of the two Fe atoms in the active site of all FPDs, except the one from *D. gigas*, where it is stabilized in a non-bonding "out" conformation. This difference was originally proposed (14) to account for the different specificity displayed by FPDs toward O₂ or NO: indeed, contrary to FDP_{Mt} (13), the *D. gigas* enzyme consumes O₂ more efficiently than NO (7). However, the recently solved structure of FDP_{Mm} (16) together with the one of the *Giardia* enzyme herein presented makes this hypothesis very unlikely. These two enzymes have a prevalent specificity for O₂, being unable to efficiently metabolize NO; nonetheless, they display the above mentioned histidine residue His-90

liganded to Fe, like the enzyme from *M. thermoacetica*, which efficiently reduces NO to N₂O (14).

More recently, Seedorf *et al.* (16) proposed that the ability of FDP_{Mm} to process only O₂ (and not NO) could be attributed to two residues, Phe-198 and Tyr-25 (according to numbering of the FDP_{Mm} enzyme), strictly conserved in FPDs from methanogenic Archaea. According to these authors Phe-198 is replaced by a Tyr and Tyr-25 by a Phe in those FPDs that are able to react not only with O₂, but also with NO. Hence, the suggestion that Phe-198 and Tyr-25 may be crucial for the O₂ specificity. However, since in FDP_{Gi} the latter residues are replaced by Tyr-199 and Phe-30 respectively, and this enzyme, like FDP_{Mm}, displays a high reactivity with O₂ but no NO-reductase activity, this hypothesis may have to be abandoned, leaving open the issue of the O₂ versus NO specificity of FPDs.

It is also important to discover the physiological reducing substrate of the FPD enzyme in *Giardia*. According to the classification of FPDs proposed by Saraiva *et al.* (3), FDP_{Gi} belongs to class A. Most of the FPDs of this class use rubredoxin as the reducing substrate, although in *M. thermoacetica* the latter protein is fused to a NAD(P)H:flavin oxidoreductase module in a single polypeptide chain, which was thus named "high molecular weight rubredoxin" (13). A notable exception is the archaeal enzyme from *M. marburgensis*, which accepts electrons from coenzyme F₄₂₀, a 5-deazaflavin derivative present in relatively high concentrations in methanogenic archaea (15). As originally noticed by Seedorf *et al.* (16), in contrast to the F₄₂₀-dependent enzymes, the FPDs using rubredoxin as the reducing substrate display a tryptophan residue stacked with the FMN cofactor, possibly involved in shuttling electrons between rubredoxin and FMN. Similarly to the other rubredoxin-dependent FPDs from *D. gigas* and *M. thermoacetica*, the latter residue (W352) is present and topologically conserved also in the *Giardia* enzyme. In analogy with FDP_{Dg} and FDP_{Mm}, Trp-352 is suitably solvent accessible and surrounded by several positively charged residues on the surface, that are likely involved in substrate recognition. Based on these structural similarities and on the ability of FDP_{Gi} to be promptly reduced by the rubredoxin domain truncated from *E. coli* FIRd, rubredoxin seems a likely candidate substrate for FDP_{Gi}, though as yet it remains to be detected in *Giardia*.

In conclusion, in the present study the first eukaryotic FDP from the human protozoan pathogen *G. intestinalis* proved to efficiently scavenge O₂, thus appearing a good candidate to promote *Giardia* survival in the small intestine. The hypothesis, if validated by direct experiments on the parasites, might provide clues to alternative therapeutic strategies in the treatment of giardiasis.

Acknowledgments—We thank the European Synchrotron Radiation Facility (Grenoble, France) for beam time allocation and technical support. We thank M. Teixeira and J. B. Vicente (Instituto de Tecnologia Quimica e Biologica, Universidade Nova de Lisboa, Lisbon, Portugal) for helpful discussions and for kindly providing the NADH:flavorubredoxin oxidoreductase and the genetically truncated rubredoxin domain of flavorubredoxin purified from *E. coli*.

⁶ A. Giuffrè, manuscript to be published.

REFERENCES

1. Wasserfallen, A., Ragetti, S., Jouanneau, Y., and Leisinger, T. (1998) *Eur. J. Biochem.* **254**, 325–332
2. Gardner, A. M., Helmick, R. A., and Gardner, P. R. (2002) *J. Biol. Chem.* **277**, 8172–8177
3. Saraiva, L. M., Vicente, J. B., and Teixeira, M. (2004) *Adv. Microb. Physiol.* **49**, 77–129
4. Chen, L., Liu, M. Y., LeGall, J., Fareleira, P., Santos, H., and Xavier, A. V. (1993) *Biochem. Biophys. Res. Commun.* **193**, 100–105
5. Gomes, C. M., Silva, G., Oliveira, S., LeGall, J., Liu, M. Y., Xavier, A. V., Rodrigues-Pousada, C., and Teixeira, M. (1997) *J. Biol. Chem.* **272**, 22502–22508
6. Frazao, C., Silva, G., Gomes, C. M., Matias, P., Coelho, R., Sieker, L., Macedo, S., Liu, M. Y., Oliveira, S., Teixeira, M., Xavier, A. V., Rodrigues-Pousada, C., Carrondo, M. A., and Le Gall, J. (2000) *Nat. Struct. Biol.* **7**, 1041–1045
7. Rodrigues, R., Vicente, J. B., Felix, R., Oliveira, S., Teixeira, M., and Rodrigues-Pousada, C. (2006) *J. Bacteriol.* **188**, 2745–2751
8. Gomes, C. M., Vicente, J. B., Wasserfallen, A., and Teixeira, M. (2000) *Biochemistry* **39**, 16230–16237
9. Gomes, C. M., Giuffre, A., Forte, E., Vicente, J. B., Saraiva, L. M., Brunori, M., and Teixeira, M. (2002) *J. Biol. Chem.* **277**, 25273–25276
10. Vicente, J. B., and Teixeira, M. (2005) *J. Biol. Chem.* **280**, 34599–34608
11. Vicente, J. B., Scandurra, F. M., Rodrigues, J. V., Brunori, M., Sarti, P., Teixeira, M., and Giuffre, A. (2007) *Febs J.* **274**, 677–686
12. Silaghi-Dumitrescu, R., Ng, K. Y., Viswanathan, R., and Kurtz, D. M., Jr. (2005) *Biochemistry* **44**, 3572–3579
13. Silaghi-Dumitrescu, R., Coulter, E. D., Das, A., Ljungdahl, L. G., Jameson, G. N., Huynh, B. H., and Kurtz, D. M., Jr. (2003) *Biochemistry* **42**, 2806–2815
14. Silaghi-Dumitrescu, R., Kurtz, D. M., Jr., Ljungdahl, L. G., and Lanzilotta, W. N. (2005) *Biochemistry* **44**, 6492–6501
15. Seedorf, H., Dreisbach, A., Hedderich, R., Shima, S., and Thauer, R. K. (2004) *Arch. Microbiol.* **182**, 126–137
16. Seedorf, H., Hagemeyer, C. H., Shima, S., Thauer, R. K., Warkentin, E., and Ermler, U. (2007) *Febs J.* **274**, 1588–1599
17. Fang, F. C. (1997) *J. Clin. Investig.* **99**, 2818–2825
18. MacMicking, J., Xie, Q. W., and Nathan, C. (1997) *Annu. Rev. Immunol.* **15**, 323–350
19. Andersson, J. O., Sjogren, A. M., Davis, L. A., Embley, T. M., and Roger, A. J. (2003) *Curr. Biol.* **13**, 94–104
20. Loftus, B., Anderson, I., Davies, R., Alsmark, U. C., Samuelson, J., Amedeo, P., Roncaglia, P., Berriman, M., Hirt, R. P., Mann, B. J., Nozaki, T., Suh, B., Pop, M., Duchene, M., Ackers, J., Tannich, E., Leippe, M., Hofer, M., Bruchhaus, I., Willhoest, U., Bhattacharya, A., Chillingworth, T., Churcher, C., Hance, Z., Harris, B., Harris, D., Jagels, K., Moule, S., Mungall, K., Ormond, D., Squares, R., Whitehead, S., Quail, M. A., Rabbinowitsch, E., Norbertczak, H., Price, C., Wang, Z., Guillen, N., Gilchrist, C., Stroup, S. E., Bhattacharya, S., Lohia, A., Foster, P. G., Sicheritz-Ponten, T., Weber, C., Singh, U., Mukherjee, C., El-Sayed, N. M., Petri, W. A., Jr., Clark, C. G., Embley, T. M., Barrell, B., Fraser, C. M., and Hall, N. (2005) *Nature* **433**, 865–868
21. Andersson, J. O., Hirt, R. P., Foster, P. G., and Roger, A. J. (2006) *BMC Evol. Biol.* **6**, 27
22. Sarti, P., Fiori, P. L., Forte, E., Rappelli, P., Teixeira, M., Mastronicola, D., Sanci, G., Giuffre, A., and Brunori, M. (2004) *Cell Mol. Life Sci.* **61**, 618–623
23. Roxstrom-Lindquist, K., Palm, D., Reiner, D., Ringqvist, E., and Svard, S. G. (2006) *Trends Parasitol.* **22**, 26–31
24. Morrison, H. G., McArthur, A. G., Gillin, F. D., Aley, S. B., Adam, R. D., Olsen, G. J., Best, A. A., Cande, W. Z., Chen, F., Cipriano, M. J., Davids, B. J., Dawson, S. C., Elmendorf, H. G., Hehl, A. B., Holder, M. E., Huse, S. M., Kim, U. U., Lasek-Nesselquist, E., Manning, G., Nigam, A., Nixon, J. E., Palm, D., Passamaneck, N. E., Prabhu, A., Reich, C. I., Reiner, D. S., Samuelson, J., Svard, S. G., and Sogin, M. L. (2007) *Science* **317**, 1921–1926
25. Brown, D. M., Upcroft, J. A., Edwards, M. R., and Upcroft, P. (1998) *Int. J. Parasitol.* **28**, 149–164
26. Brown, D. M., Upcroft, J. A., and Upcroft, P. (1995) *Mol. Biochem. Parasitol.* **72**, 47–56
27. Brown, D. M., Upcroft, J. A., and Upcroft, P. (1996) *Eur. J. Biochem.* **241**, 155–161
28. Smith, P. K., Krohn, R. I., Hermanson, G. T., Mallia, A. K., Gartner, F. H., Provenzano, M. D., Fujimoto, E. K., Goeke, N. M., Olson, B. J., and Klenk, D. C. (1985) *Anal. Biochem.* **150**, 76–85
29. Susin, S., Abian, J., Sanchez-Baeza, F., Peleato, M. L., Abadia, A., Gelpi, E., and Abadia, J. (1993) *J. Biol. Chem.* **268**, 20958–20965
30. Stoeckley, L. L. (1970) *Anal. Chem.* **42**, 779–781
31. Otwinowski, Z., and Minor, W. (eds) (1997) *Methods in Enzymology* (Carter, C. W., and Sweet, R. M., eds) Academic Press, New York
32. Vagin, A., and Teplyakov, A. (1997) *J. Appl. Crystallogr.* **30**, 1022–1025
33. Murshudov, G. N., Vagin, A. A., and Dodson, E. J. (1997) *Acta Crystallogr. D Biol. Crystallogr.* **53**, 240–255
34. Emsley, P., and Cowtan, K. (2004) *Acta Crystallogr. D Biol. Crystallogr.* **60**, 2126–2132
35. Laskowski, R. R., MacArthur, M. W., Moss, D. S., and Thornton, J. M. (1993) *J. Appl. Crystallogr.* **26**, 283–291
36. Krissinel, E., and Henrick, K. (2004) *Acta Crystallogr. D Biol. Crystallogr.* **60**, 2256–2268
37. Sobolev, V., Sorokine, A., Prilusky, J., Abola, E. E., and Edelman, M. (1999) *Bioinformatics* **15**, 327–332
38. Lee, B., and Richards, F. M. (1971) *J. Mol. Biol.* **55**, 379–400
39. Solomon, E. I., Brunold, T. C., Davis, M. I., Kemsley, J. N., Lee, S. K., Lehnert, N., Neese, F., Skulan, A. J., Yang, Y. S., and Zhou, J. (2000) *Chem. Rev.* **100**, 235–350
40. Lloyd, D., Harris, J. C., Maroulis, S., Biagini, G. A., Wadley, R. B., Turner, M. P., and Edwards, M. R. (2000) *Microbiology* **146**, 3109–3118
41. Townson, S. M., Upcroft, J. A., and Upcroft, P. (1996) *Mol. Biochem. Parasitol.* **79**, 183–193
42. Li, L., and Wang, C. C. (2006) *Mol. Microbiol.* **59**, 202–211
43. Sheridan, W. G., Lowndes, R. H., and Young, H. L. (1990) *Am. J. Surg.* **159**, 314–319
44. Paget, T. A., Jarroll, E. L., Manning, P., Lindmark, D. G., and Lloyd, D. (1989) *J. Gen. Microbiol.* **135**, 145–154
45. Ellis, J. E., Wingfield, J. M., Cole, D., Boreham, P. F., and Lloyd, D. (1993) *Int. J. Parasitol.* **23**, 35–39
46. Eckmann, L., Laurent, F., Langford, T. D., Hetsko, M. L., Smith, J. R., Kagnoff, M. F., and Gillin, F. D. (2000) *J. Immunol.* **164**, 1478–1487
47. Li, E., Zhou, P., and Singer, S. M. (2006) *J. Immunol.* **176**, 516–521

The O₂-scavenging Flavodiiron Protein in the Human Parasite *Giardia intestinalis*
Adele Di Matteo, Francesca Maria Scandurra, Fabrizio Testa, Elena Forte, Paolo Sarti,
Maurizio Brunori and Alessandro Giuffrè

J. Biol. Chem. 2008, 283:4061-4068.

doi: 10.1074/jbc.M705605200 originally published online December 12, 2007

Access the most updated version of this article at doi: [10.1074/jbc.M705605200](https://doi.org/10.1074/jbc.M705605200)

Alerts:

- [When this article is cited](#)
- [When a correction for this article is posted](#)

[Click here](#) to choose from all of JBC's e-mail alerts

Supplemental material:

<http://www.jbc.org/content/suppl/2007/12/12/M705605200.DC1>

This article cites 46 references, 9 of which can be accessed free at
<http://www.jbc.org/content/283/7/4061.full.html#ref-list-1>